Front. Phys. China, 2010, 5(3): 319–323
DOI 10.1007/s11467-010-0010-1

RESEARCH ARTICLE

A broadband simplified free space cloak realized by nonmagnetic dielectric cylinders

Di BAO (鲍迪)[1], **Efthymios KALLOS**[1], **Wen-xuan TANG** (汤文轩)[1], **Christos ARGYROPOULOS**[1], **Yang HAO** (郝阳)[1,†], **Tie-jun CUI** (崔铁军)[2]

[1] *Department of Electronic Engineering, Queen Mary, University of London, Mile End Road, London, E1 4NS, UK*
[2] *State Key Laboratory of Millimeter Waves, Department of Radio Engineering, Southeast University, Nanjing 210096, China*
E-mail: yang.hao@elec.qmul.ac.uk

Received February 2, 2010; accepted March 12, 2010

In this paper, the properties of cylindrical high permittivity dielectric particles are studied. A design for broadband reduction of the scattering signature of metallic objects is proposed by implementing simplified ground-plane cloaking schemes. The devices are functional in the presence of a ground plane as well as in free space ranging from 4 GHz to 10 GHz. The required dielectric map for the cloak is achieved by means of manipulating the dimensions of the periodically distributed dielectric cylinders embedded in a host medium with a permittivity close to one. The scattering reduction effects are verified through simulation results. The proposed all dielectric cloaks are advantageous over other schemes due to their non-dispersive nature, the broad bandwidth, the low loss, and the ease of fabrication.

Keywords cloak, dielectric cylinders, FFT, gradient index material

PACS numbers 41.20.Jb

1 Introduction

The invisibility cloak has attracted increasing attention in the past few years since it was proposed [1]. Although an experimental verification was carried out at microwave frequencies [2], earlier designs of free-space cloaks suffered from inherent limitations of metamaterials, such as high loss and narrow bandwidth. Li *et al.* proposed a so-called ground-plane cloak design [3], which makes broadband cloaking feasible. The idea has been experimentally verified at both microwave and infrared frequencies [4–7]. However, these designs require high index background materials, which contain a very large number of metamaterial cells. Subsequently, the idea of the quasi-cloak, which consists of a few carefully designed all-dielectric blocks was presented in Ref. [8]. The quasi-cloak completely removes the constrains of metamaterials without significantly sacrificing its performance. Thus, it enables certain practical applications from microwave to optical frequency band.

A variety of methods can be used to construct the quasi-cloak. For example, in the printed circuit board (PCB) method, I-shaped metal structures are used on PCBs with F4B substrates [7]. Utilizing electron beam lithography, arrays of silicon nanorods can be fabricated to achieve gradient indices [9]. Using dielectric mixing, composites with nonmagnetic particles are dispersed in a polymer matrix. Cylindrical metallic post surface-wave structures and holey plate structures have also been utilized in the design of gradient index lenses, such as the Luneburg Lens [10, 11].

In this work, we examine the use of periodic arrays of high-index dielectric cylinders operating off-resonance at microwave frequencies in order to achieve low-loss broadband materials with gradient refractive indices. The properties of such effective media consisting of arrays of dielectric particles were first studied in the literature in Refs. [12, 13]. Several methods have been proposed for the retrieval of the effective parameters based on measured or simulated S parameters [14, 15]. In this paper, the effective refractive index of arrays of cylinders is evaluated using a Fourier transform method to extract the spatial wavelength of the electric field inside the arrays for different setups, and the results are compared with a conventional S parameter retrieval method, which is based on the effective medium theory [14]. We then demonstrate the operation of the simplified ground-plane cloak constructed from such dielectric cylinders via numerical simulations. The proposed device operates as a ground-plane cloak when placed on top of a ground plane, and in addition, it can be modified into a direc-

tional free-space cloak that significantly reduces the scattering from an impinging plane wave at certain angles. Since those designs do not require to be embedded in background media, they remain compact and simple to build. The techniques presented here are generic and can be applied to the design of other devices obtained via transformation electromagnetics [16–18].

2 Properties of dielectric cylinders

In this section, we examine in detail the effective electromagnetic properties of the dielectric cylinder arrays. The dielectric cylinders of interest in this paper are assumed to have a permittivity equal to 36.7 and a radius of 1.5 mm. The specific permittivity values are chosen because of its availability of dielectric materials, for example, $(Z_r, S_n)TiO_4$ ceramics as main ingredients. By placing the cylinders in a periodic array between two-plated waveguide and varying their height between 0.1 mm and 3 mm, one can obtain different effective indices with values between 1.02 and 1.49 at microwave frequencies.

We apply two different methods in order to calculate the effective refractive index, with the aid of finite element method simulations (Ansoft HFSS). First, the FFT method is applied to calculate the effective parameters of the structure. In the FFT method, a periodic array of dielectric cylinders, as shown in Fig. 1(a), is simulated at 5 GHz to derive the spatial frequency component of the electric field amplitude distribution inside the array along the wave propagation direction ($+y$ axis). The cylinders have height equal to 1.7 mm, radius 1.5 mm, and permittivity of 36.7 and are excited by TM waves. The two-dimensional electric field distribution in free space is shown in Fig. 1(b), and the corresponding field distribution of the array of cylinders is shown in Fig. 1(c). The magnitude of the electric field distributions along the y direction in Fig. 1(b) and (c) are

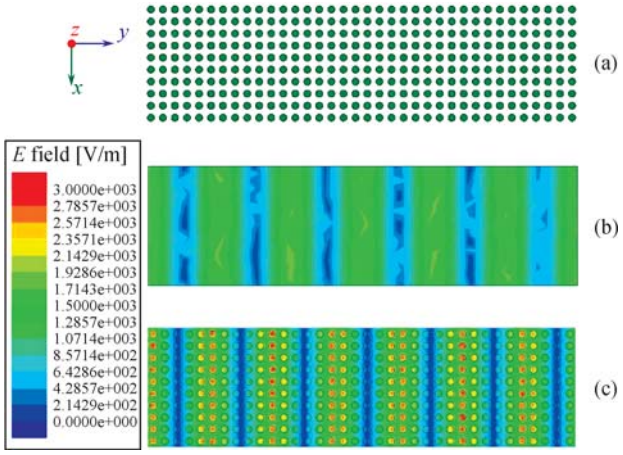

Fig. 1 **(a)** The dielectric disc matrix. **(b)** The electric field distribution in free space. **(c)** The electric field distribution in the dielectric disc matrix.

depicted in Fig. 2(a). Comparing these two cases, it is evident that the wavelength is compressed inside the array, which indicates that the medium has a refractive index larger than one. In order to quantify the wavelength compression, we obtain the Fourier Transforms of the electric field lineouts of Fig. 2(a) and plot them in Fig. 2(b). We observe that besides the DC component, there are strong peaks, which correspond to the spatial frequency components. By measuring the resulting spatial frequency, the refractive index can be evaluated as:

$$n \simeq f_s/f_0 \tag{1}$$

where f_0 is the spatial frequency of free space, f_s is the spatial frequency of the cylinder matrix, and n is effective refractive index. In this particular case, $f_0 \simeq 34\,\mathrm{m}^{-1}$ and $f_s \simeq 38.33\,\mathrm{m}^{-1}$, thus $n \simeq 1.13$.

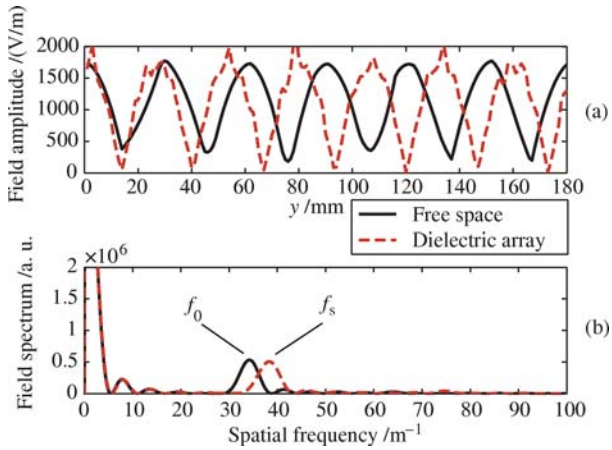

Fig. 2 **(a)** The electric field distribution alone y axis in free space (*red line*) and dielectric disc matrix (*blue line*). **(b)** The FFT of the electric field distribution.

In order to verify these results,the S-parameter retrieval method is also used to calculate the refractive index of different cylinders at a frequency of 5 GHz with the cylinders placed in a cubic lattice with a period of 5 mm. The refractive index and impedance can be directly calculated from the reflection and transmission coefficients assuming excitation by waveports [19].

The results using both methods to evaluate the refractive index for various setups are shown in Fig. 3. The extracted effective refractive indices as a function of their height for an array of periodic cylinders with three different lattice periods in the x–y plane, are compared in Fig. 3(a). This demonstrates that an almost continuous range of indices between 1.02 and 1.49 can be obtained by tuning parameters, such as the height and period of dielectric cylinders.

Figure 3 also shows that the two methods yield similar results for a lattice period equal to 5 mm, although the permittivity values in the FFT method are slightly higher than those obtained with S-parameter retrieval for cylinders with larger heights, as Fig. 3(a) suggests. The small discrepancy is probably caused by not consid-

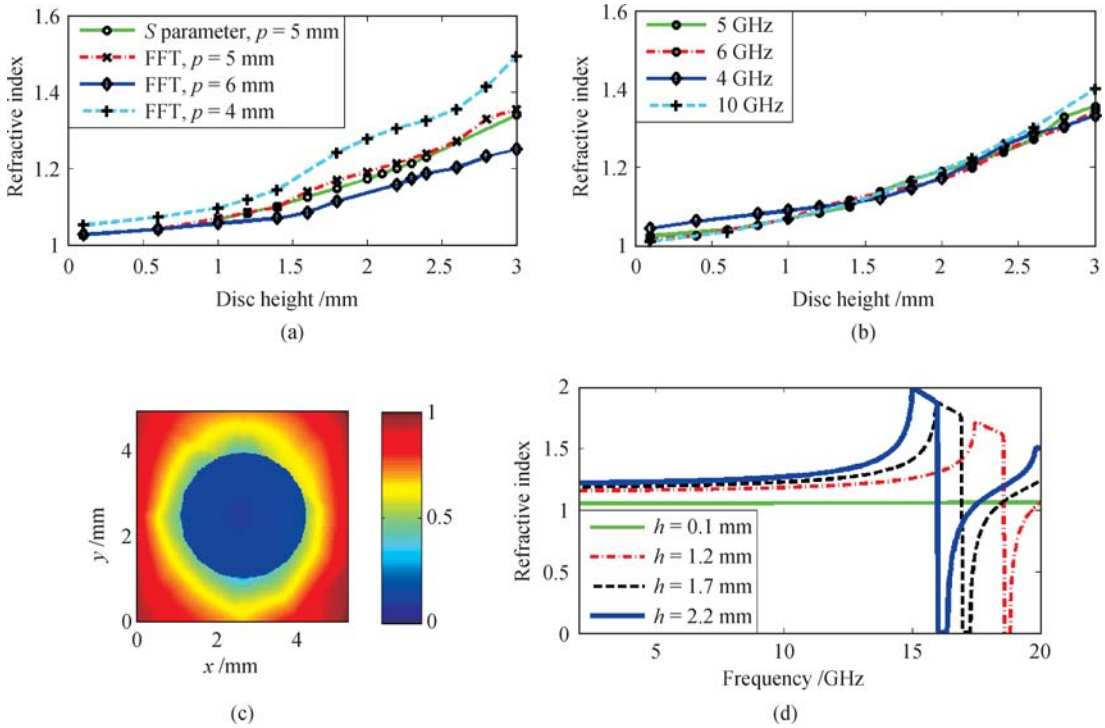

Fig. 3 **(a)** Calculated effective refractive index using the FFT and the S-parameter retrieval methods for cylinder arrays with different spatial periods at 5 GHz. p is the period in x and y axis, while the period in z axis is 5 mm. **(b)** Calculated effective refractive index of the cylinder array using the FFT method at different frequencies and a period of 5 mm. **(c)** The normalized electric field distribution in the vicinity of a 2.2-mm-tall dielectric cylinder at the off resonant frequency of 5 GHz. **(d)** Calculated effective refractive index as a function of frequency using the S-parameter method and a period of 5 mm, for different cylinder heights.

ering any coupling effects in the S-parameter retrieval method. In the rest of the paper, the design of the cylinders is based on the results obtained with the FFT method. The difference between the curves with different period also indicate that cylinders with different density can also be used to construct gradient index structures.

Figure 3(b) shows the broadband response of the array of cylinders around the frequency of interest. The index as a function of the cylinders height is shown at different frequencies: 4 GHz, 5 GHz, 6 GHz, and 10 GHz. The maximum deviation is less than 4 % within the above frequency range for the dielectric cylinder arrays with all different heights investigated here. This demonstrates its broadband nature of "artificial dielectrics" formed by discrete dielectric cylinders operating at off-resonance frequencies: for example, the lowest resonant frequency of the dielectric cylinders is around 17.1 GHz, for a given height of 2.2 mm and a radius of 1.5 mm. While the resonant modes of a cylinder produce magnetic field distributions concentrated mostly inside the structure [20], at off-resonance frequencies, (i.e., 5 GHz), little field penetrates inside the high-index dielectric, as shown in Fig. 3(c), for TM plane wave incidence.

Furthermore, the frequency response of the refractive index evaluated using the S-parameter method with a lattice period of 5 mm for four different heights is shown in Fig. 3(d). We observe that below 10 GHz, where the cylinders operate off resonance, the effective refractive index indeed varies only slightly.

3 Design examples using high index dielectric cylinders

Based on the simplified ground-plane cloaking design [8], a cover structure is designed to reduce scattering from a triangular-shaped object with its base placed on a perfectly conducting metallic plane. The object has a height of 16 mm, base of 144 mm, and thickness of 5 mm (see Fig. 4). The device extends 137 mm by 60 mm around the object and consists of eight different sections, each with a different refractive index: [1.08, 1.14, 1.01, 1.21]. In order to obtain these values, one layer of dielectric cylinders is placed around the device at a period of 5 mm, while their heights are tuned to the values [1.2, 1.7, 0.1, 2.2] mm, as shown schematically in Fig. 4. The heights of the cylinders are chosen such that the corresponding effective refractive index values are obtained, according to Fig. 3(a). Each of the eight blocks consists of 7×6 identical cylinders. Some cylinders have been omitted to fit the structure around the object, for a total of 280 dielectric particles. In an experimental scenario, the cylinders can be mounted on a thin layer of foam with a refractive index close to 1.

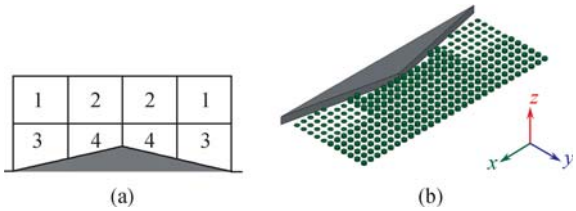

Fig. 4 **(a)** Top view of the cloak. The blocks with the same number have the same parameters. $n_1 = 1.08$, $n_2 = 1.14$, $n_3 = 1.01$, and $n_4 = 1.21$. **(b)** Perspective view of the metallic object and the cover of cylinder arrays. The lattice period is 5 mm.

The simulation results of the electric field amplitude distribution at an operating frequency of 5 GHz are shown in Fig. 5. A 30-cm wide TM pulse is incident at 45 degrees from the left side of the device. The results when there is no object [Fig. 5(a)], for the bare metallic object on the ground plane [Fig. 5(b)], and with the covered object [Fig. 5(c)] are shown. In Fig. 5(b), with the presence of the bare triangular-shaped bump, the incident wave is strongly scattered and split into two beams. In Fig. 5(c), the reflected wave is almost the same as the one in Fig. 5(a), where no object is present. Therefore, the device can successfully restore the field that is disturbed by the bare object. In addition, a detailed electric field distribution near the object and the structure is shown in Fig. 5(d). It is observed that the electric field indeed does not penetrate inside the dielectric cylinders and illustrates that the wave perceives each lattice region as a nearly homogeneous material.

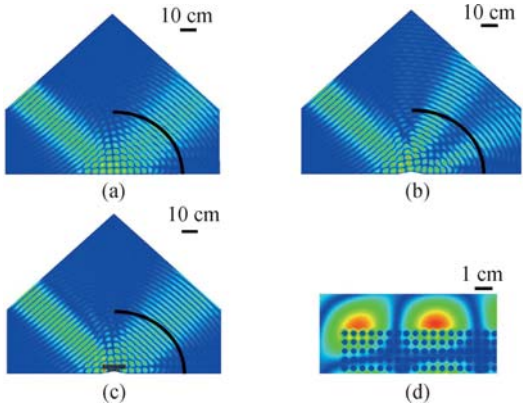

Fig. 5 Simulation results of the cloaking device at 5 GHz when **(a)** a plane wave is incident on the ground plane, **(b)** a plane wave is incident on the metallic object placed on the ground plane, and **(c)** a plane wave incident on the object covered with the structure of Fig. 4. **(d)** Detail field distribution of the covered object. The black curves indicate the locations where the field is recorded.

In order to quantitatively evaluate the performance of the device, the angular distribution of the scattered field energy at a half-circle is shown in Fig. 6. When the field scatters off the bare object, two strong sidelobes are observed (*black line*). However, when the device made from the dielectric cylinders is placed around the object (*red line*), the field pattern of scattering from a ground plane (*blue line*) is restored. We also notice that the performance of the solid dielectrics (*green line*) is almost the same as the one with dielectric cylinders, which demonstrates that the dielectric cylinders work perfectly as an effectively continuous medium. Similar behavior is observed when the impinging wave frequency is tuned to 10 GHz (*dark green line*), demonstrating the broadband capabilities of the device. Beyond 10 GHz, the performance of the device deteriorates because of the frequency dispersion caused by the cylinder's inherent resonance [Fig. 3(d)].

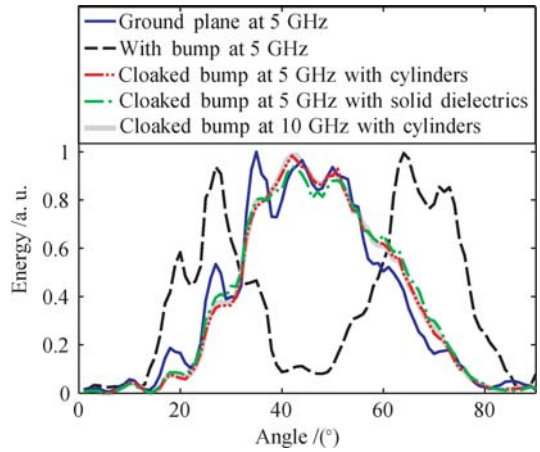

Fig. 6 Angular distribution of the scattered field energy, as recorded along the black curves shown in Fig. 5.

Next, a device is designed to operate in free space without a ground plane present by mirroring the object and the cover symmetrically around its base. For a wave incident parallel to the long axis of the device, the scattering signature of the metallic object is expected to be significantly reduced because the wave would perceive the whole structure as a thin metal sheet [8]. The simulation results for this setup are shown in Fig. 7. The electric field distribution in Fig. 7(a) shows that, at 5 GHz, the plane wave splits into two beams and creates a strong shadow behind the bare diamond-shaped object. In Fig. 7(b), where the cover is placed around the object, it is clear that the device constructed from dielectric cylinders restores the previously distorted field and greatly reduces unwanted scattering. The scattering reduction effect is less pronounced compared to the ground-plane case, because for all practical purposes there will always be some unwanted scattering from the simplified 8-block design of the cover, which in this setup is enhanced by the sharp front tip of the object. However, this can be improved if less sharp objects are used or if a more detailed cover is utilized. The main point of the results presented here is to demonstrate the effectiveness of using the dielectric cylinder arrays to construct such a structure. Finally, other simulation results (not shown here) also indicate that the device operates properly up to 10 GHz, as is the case for the ground plane setup in Fig. 5.

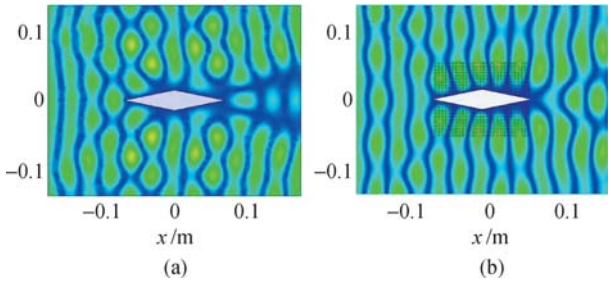

Fig. 7 Simulation results of the structure embedded in free space at 5 GHz. **(a)** Plane wave incident on the bare diamond-shaped metallic object. **(b)** Plane wave incident on the object covered with the array of cylinders.

4 Conclusion

Summarizing, a physical and explicit design of a broadband cloaking mechanism built from only four unique blocks of periodic arrays of high-index dielectric cylinders has been presented. A Fourier Transform method is adopted to calculate the effective refractive index of the arrays, and it is compared to a conventional parameter retrieval method. Simulation results demonstrate that the arrays operate as an effective continuous medium with a geometry-dependent refractive index within a very broad range of microwave frequencies. We numerically demonstrate examples where scattering from metallic objects, either placed on a ground plane or suspended in free space, can be reduced by one order of magnitude in a broadband and non-resonant fashion. The proposed all dielectric devices can be realized experimentally since the structure is fairly simple, and there is no need of background materials. The dielectric cylinders have potential applications in three-dimensional structure design. Similar techniques could be applied to design gradient index materials for other applications.

Acknowledgements This work was supported by China Scholarship Council.

References

1. J. B. Pendry, D. Schurig, and D. R. Smith, Science, 2006, 312: 1780
2. D. Schurig, J. J. Mock, B. J. Justice, S. A. Cummer, J. B. Pendry, A. F. Starr, and D. R. Smith, Science, 2006, 314: 977980
3. J. Li and J. Pendry, Phy. Rev. Lett., 2008, 101: 203901
4. R. Liu, C. Ji, J. J. Mock, J. Y. Chin, T. J. Cui, and D. R. Smith, Science, 2009, 323: 366
5. T. Z. G. B. Jason Valentine, J. Li, and X. Zhang, Nature Materials, 2009, 8(568): 10
6. L. Gabrielli, J. Cardenas, C. Poitras, and M. Lipson, Nature Photonics, 2009, 3: 461
7. H. Ma, W. Jiang, X. Yang, X. Zhou, and T. J. Cui, Opt. Express, 2009, 17: 19947
8. E. Kallos, C. Argyropoulos, and Y. Hao, Phys. Rev. A, 2009, 79: 63825
9. J. Lee, J. Blair, V. Tamma, Q. Wu, S. Rhee, C. Summers, and W. Park, Opt. Express, 2009, 17: 12922
10. C. Walter, IEEE Trans. Antennas Propag., 1960, 8: 508
11. K. Sato and H. Ujiie, Electronics & Communications in Japan, Part I: Communications (English Translation of Denshi Tsushin Gakkai Ronbunshi), 2002, 85: 1
12. L. Rayleigh, Phil. Mag., 1892, 34: 205
13. L. Lewin, J. Inst. Elec. Eng., 1947, 94: 65
14. D. Smith, D. Vier, T. Koschny, and C. Soukoulis, Phys. Rev. E, 2005, 71: 036617
15. A. Scher and E. Kuester, Metamaterials, 2009, 3: 44
16. N. Padilla, Opt. Express, 2009, 17: 14872
17. D. Roberts, N. Kundtz, and D. Smith, Opt. Express, 2009, 17: 16535
18. R. Liu, Q. Cheng, J. Chin, J. Mock, T. Cui, and D. Smith, Opt. Express, 2009, 17: 21030
19. D. Smith, S. Schultz, P. Markoš, and C. Soukoulis, Phys. Rev. B, 2002, 65: 195104
20. J. Kim and A. Gopinath, Phys. Rev. B, 2007, 76: 115126